Are polyaniline (PANI) and polypyrrole (PPy) electrocatalysts for oxygen (O_2) reduction to hydrogen peroxide (H_2O_2)?

Hannah Rabl, Dominik Wielend *, Serpil Tekoglu, Hathaichanok Seelajaroen, Helmut Neugebauer, Nikolas Heitzmann, Dogukan Hazar Apaydin†, Markus Clark Scharber, Niyazi Serdar Sariciftci

Linz Institute for Organic Solar Cells (LIOS), Institute of Physical Chemistry, Johannes Kepler University Linz, Altenberger Strasse 69, 4040 Linz, Austria.

†New address: Institute of Materials Chemistry, TU Wien, Getreidemarkt 9, 1060 Wien, Austria.

(*Email: dominik.wielend@jku.at)

Supporting information

1. Optimizing the polyaniline polymerization conditions

In order to produce fully metal-free polyaniline (PANI) films on electrodes, electrochemical oxidative polymerization, initially discovered by Letheby[1], was performed based on the conditions described by Nunziante and Pistoia[2]. The goal was, to obtain thin films of PANI which are in ideal case fully covering the whole surface, starting with the comparison of number of CV cycles performed in FigureS 1:

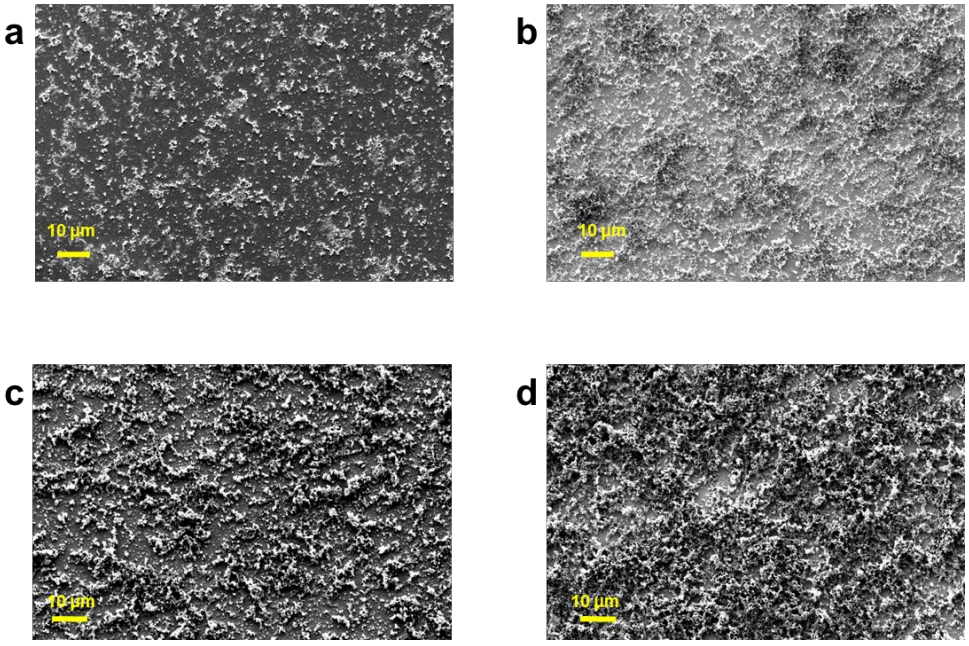

FigureS 1: Influence of the number of CV cycles upon PANI film formation performed in 0.25 M aniline solution at a scan rate of 25 mV s^{-1}. a) 4 cycles, b) 8 cycles, c) 10 cycles and d) 20 cycles.

As a next step, the concentration of aniline in the electrolyte solution was varied in order to find the best conditions:

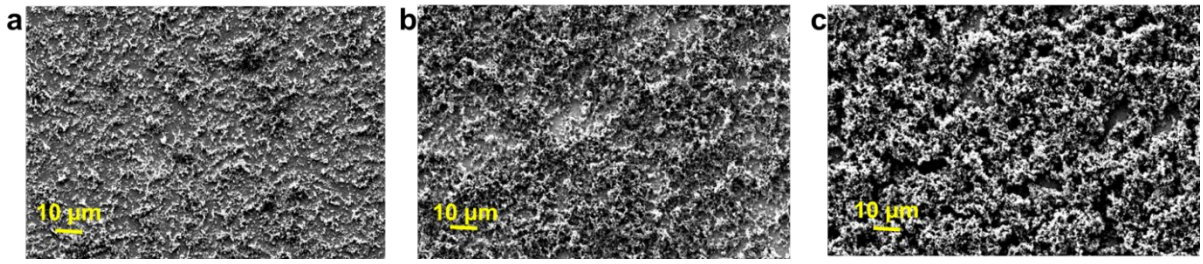

FigureS 2: Influence of the aniline concentration upon PANI film formation performed at a scan rate of 25 mV s^{-1} for 20 cycles. a) 0.1 M, b) 0.25 M and c) 0.50 M.

In the following FigureS 3 the influence of scan rate upon film morphology was investigated:

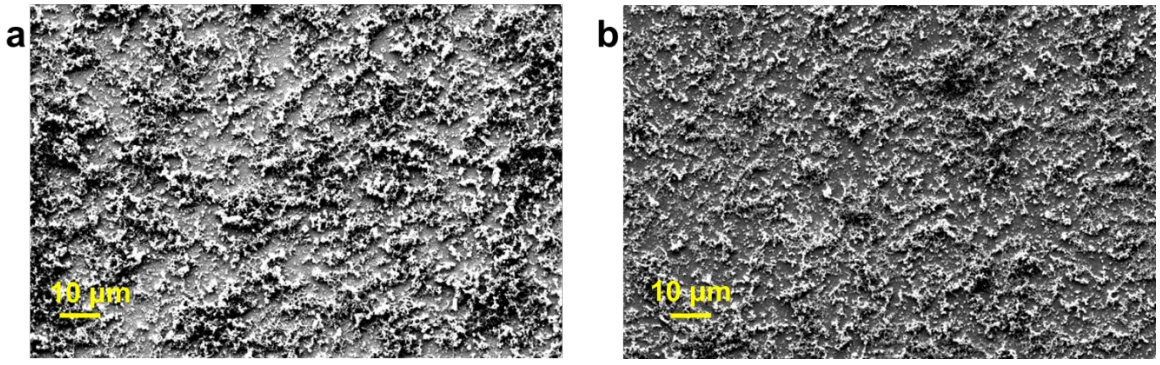

FigureS 3: Influence of the scan rate upon PANI film formation performed in 0.1 M aniline solution with 20 cycles. a) 10 mV s^{-1} and b) 25 mV s^{-1}.

In a final test, the importance of the applied potentiodynamic polymerization over constant potential polymerization was investigated. Therefore, in the following FigureS 4 the results of polymerizations kept at + 800 mV for 30 min are compared:

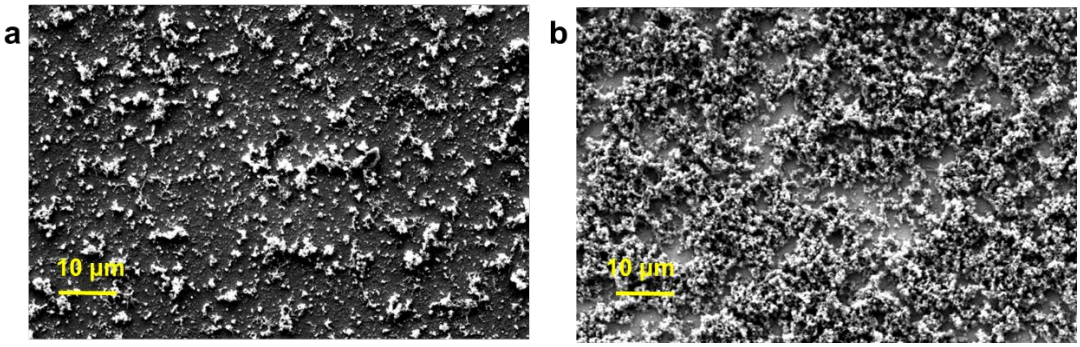

FigureS 4: Results of potentiostatic polymerization at +800 mV for 30 min in a) 0.1 M and b) 0.5 M aniline solutions.

As can be seen from FigureS 4a, the potentiostatic polymerization in 0.1 M aniline solution results in fairly poor surface coverage. Although the one in 0.5 M aniline solution showed higher surface coverage and larger film thickness, still the results from potentiodynamic polymerization in FigureS 2 showed more promising results.

2. Quantification of hydrogen peroxide (H_2O_2) produced

The quantification of H_2O_2 produced during chronoamperometry was done according to recent reports of a colorimetric detection by Su *et al.*[3] and Apaydin *et al.*[4]. To start with, a stock solution of 4 mM *p*-nitrophenyl boronic acid (*p*NBA, Sigma Aldrich) in DMSO (VWR) and a 150 mM Na_2CO_3/$NaHCO_3$ (Fluka; Sigma Aldrich) buffer solution at pH 9 in a 1:1 ratio was prepared. This solution was mixed with the samples and after 36 min reaction time under dark conditions, the absorbance values at 411 nm were recorded using a Thermo Fischer Multiskan Go Microplate Spectrophotometer. Upon calibration with H_2O_2 standard solutions (Merck) resulting in the calibration curve in FigureS 5, the amount of H_2O_2 was calculated. In order to get the required change in absorbance, the absorbance of a blank sample was subtracted.

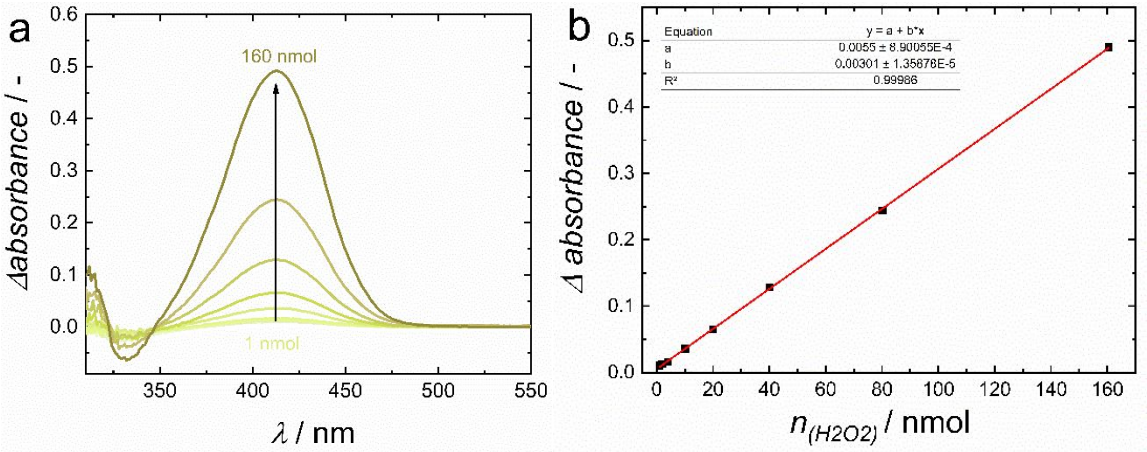

FigureS 5: a) Subtracted absorption spectra of standard H_2O_2 solutions and b) calibration curve of H_2O_2 re-calculated thereof.

3. Spectroscopic materials characterization

The spectroscopic results of ATR-FTIR and Raman spectroscopy of PANI on Cr-Au electrodes are shown in the following FigureS 6:

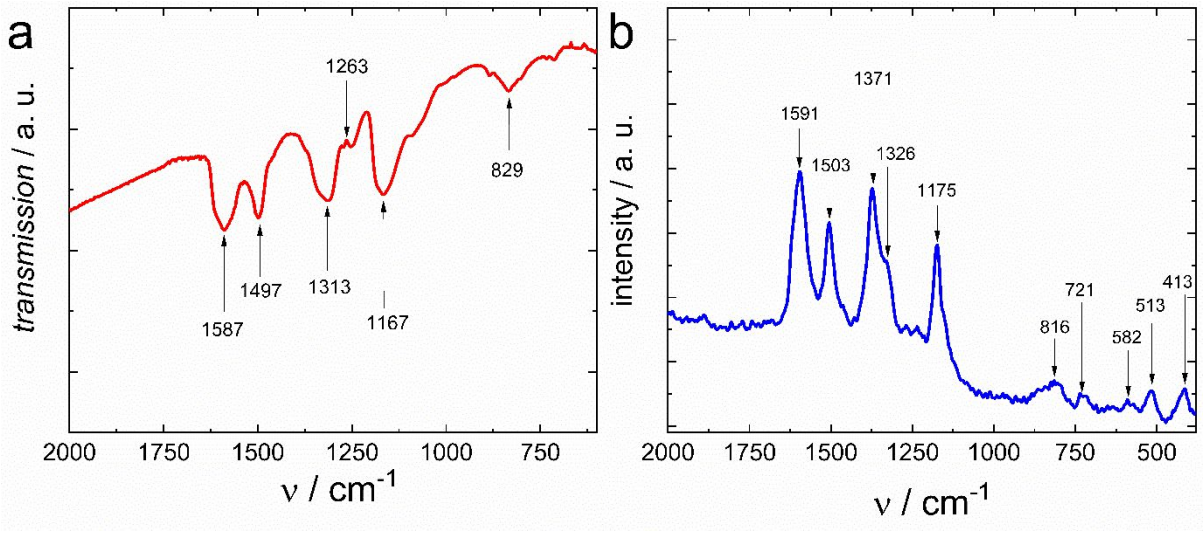

FigureS 6: a) ATR-FTIR spectrum and b) Raman spectrum of PANI.

The characteristic bands of the polyaniline base were detected and are in accordance to literature reports[5,6].

The spectroscopic results of ATR-FTIR and Raman spectroscopy of PPy on Cr-Au electrodes is shown in the following FigureS 7:

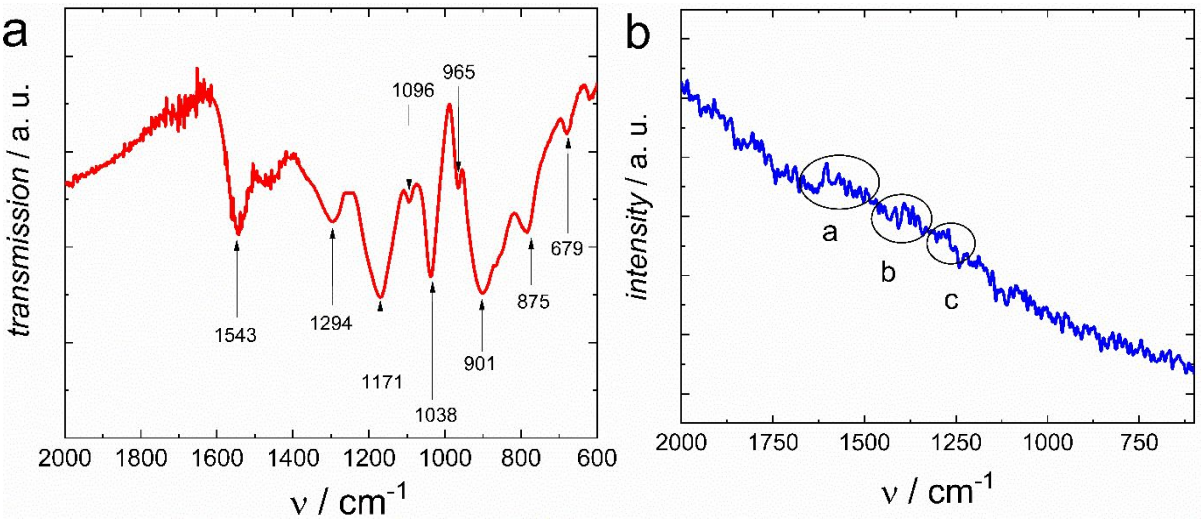

FigureS 7: a) ATR-FTIR spectrum and b) Raman spectrum of PPy.

From the FTIR, the characteristic bands of the polypyrrole base were detected and are in well accordance to literature reports[6]. The Raman spectrum of PPy only showed faint features due to instability during the laser treatment.

4. Carbon paper – SEM image characterization

In the following FigureS 8, SEM images of bare carbon paper are shown:

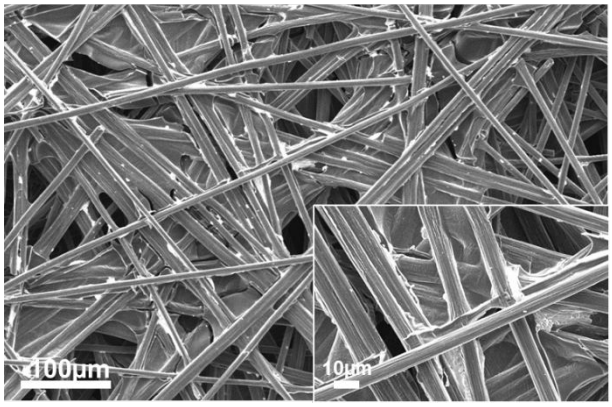

FigureS 8: SEM images of bare CP.

Similar to Figure 2c+d, the carbon fibres are visible, but they have a smooth surface structure.

5. Blank CV experiments

The following shows the CV curves of blank GC as well as blank CP:

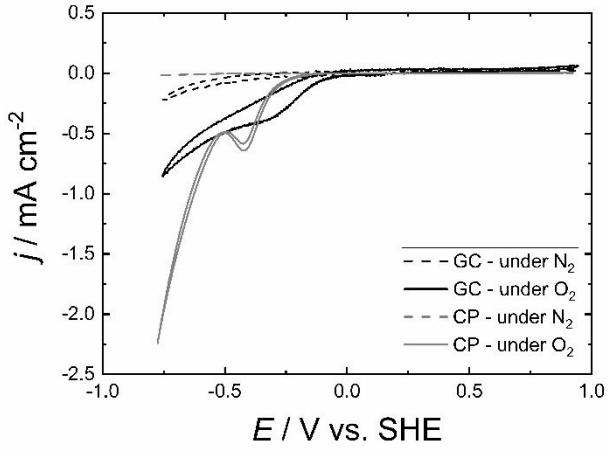

FigureS 9: CV of GC and CP w/o O_2.

As can be seen from FigureS 9, CP possessed a distinct reduction peak for ORR compared to GC, which only showed a reductive feature. Under N_2 saturated conditions, both GC and CP show nearly no electrochemical feature in the regime studied.

6. H_2O_2 production - Polyaniline

In order to determine the optimum pH medium as well as reduction potential for H_2O_2 production via chronoamperometry, three pH values and four different potentials were investigated as demonstrated in FigureS 10:

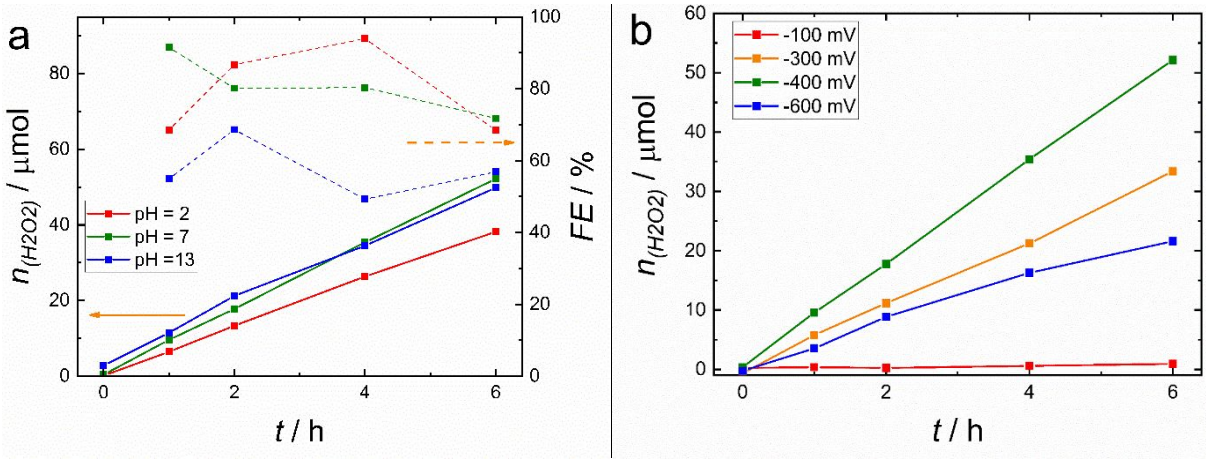

FigureS 10: Optimization of electrochemical H_2O_2 production regarding a) pH value and b) regarding applied potential vs. SHE at pH 7 using GC/PANI electrode.

Representative transient curves with accumulated charges from chronoamperometry experiments of blank GC and GC/PANI are shown in FigureS 11:

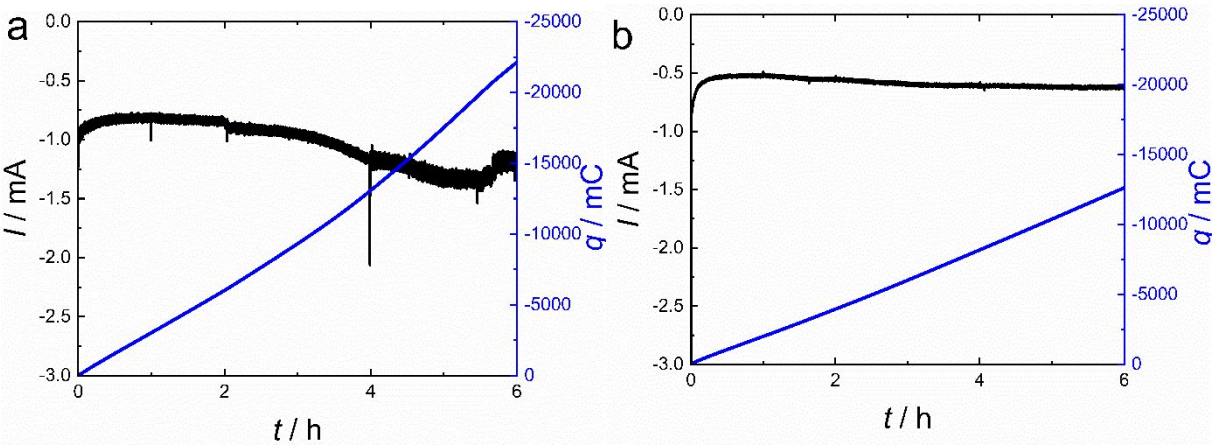

FigureS 11: Results of chronoamperometry of a) blank GC and b) GC/PANI at pH 7 at -400 mV vs. SHE.

In analogy to Figure 3, CV and chronoamperometry of GC/PANI were also performed at pH 2 as shown in FigureS 12:

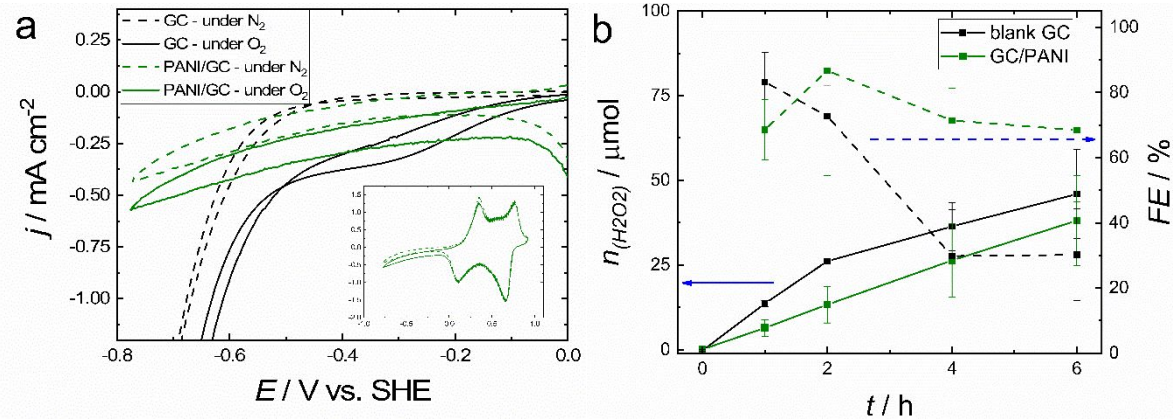

FigureS 12: a) CV of GC/PANI in 0.1 M $NaHSO_4$ w/o O_2. b) Results of chronoamperometry of blank GC as well as GC/PANI at pH 2 at -400 mV vs. SHE.

The results for H_2O_2 production using CP/PANI as well as blank CP are summarized in the following FigureS 13:

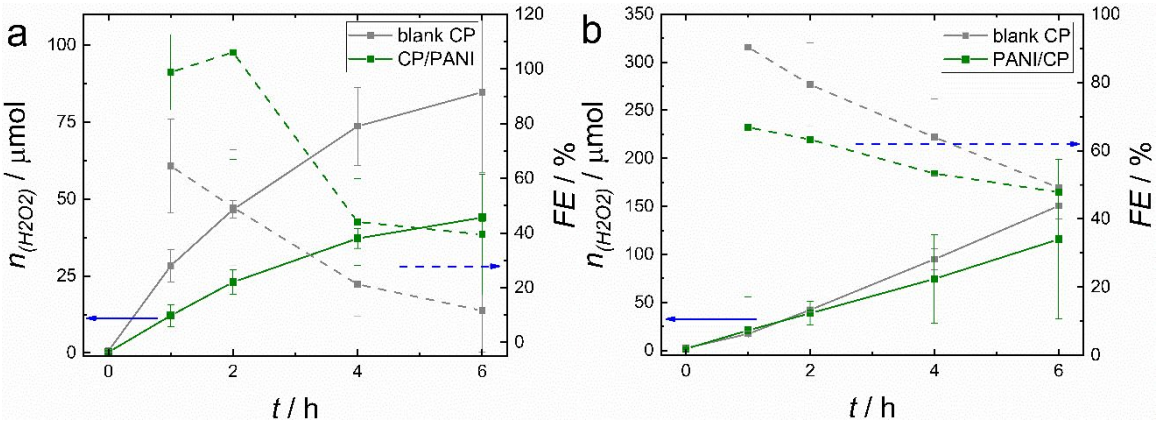

FigureS 13: a) Produced H_2O_2 and FE of CP and CP/PANI at pH 7. b) Produced H_2O_2 and FE of CP and CP/PANI at pH 2.

7. H_2O_2 production - Polypyrrole

In order to investigate polypyrrole towards electrochemical H_2O_2 production, GC/PPy and CP/PPy were investigated at pH 2, as shown in FigureS 14:

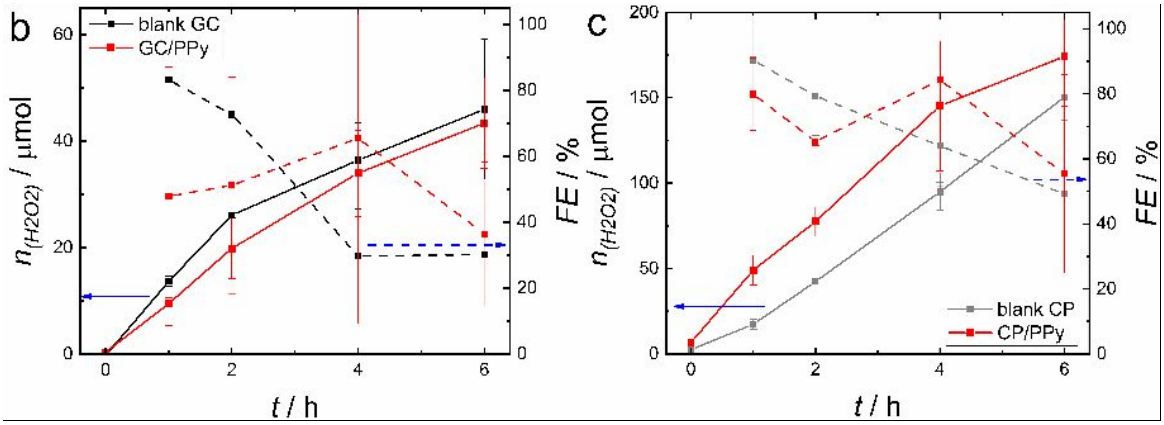

FigureS 14: a) Produced H_2O_2 and FE of GC and GC/PPy at pH 2. b) Produced H_2O_2 and FE of CP and CP/PPy at pH 2.

8. Hydrodynamic voltammetry

Hydrodynamic experiments like rotating disc electrode (RDE) or rotating ring-disc electrode (RRDE) are frequently used to compare electrocatalysts and determine the number of transferred electrons for the ORR step. The exchange current I_K and the number of transferred electrons n can be calculated by performing linear sweep voltammetry (LSV) at various rotation speed ω by applying the Koutecki-Levich-Equation[7] shown in eq. 1:

$$\frac{1}{I} = \frac{1}{I_K} + \frac{1}{0.62\, n\, F\, A\, D^{2/3}\, \upsilon^{-1/6}\, c_0} \cdot \frac{1}{\omega^{1/2}} \tag{1}$$

By investigation of RRDE, the number of transferred electrons n (eq. 2) as well as the corresponding faradaic efficiency (eq. 3) can be calculated by performing LSV at various rotation speeds from the disc current I_D and the ring current I_R[8,9]:

$$n = \frac{4 \cdot |I_D|}{|I_D| + I_R/N} \tag{2}$$

$$FE(\%) = \frac{I_R/N}{|I_D|} \cdot 100 \tag{3}$$

Both formulas in eq. 2 and eq. 3 contain the value for the collection efficiency N, which is a quantity determined by the RRDE geometry and can be determined experimentally using the following eq. 4

$$N_{exp} = \frac{I_R}{|I_D|} \tag{4}$$

when investigating a known and fast redox-active compound like $K_3[Fe(CN)_6]$ as illustrated in FigureS 15:

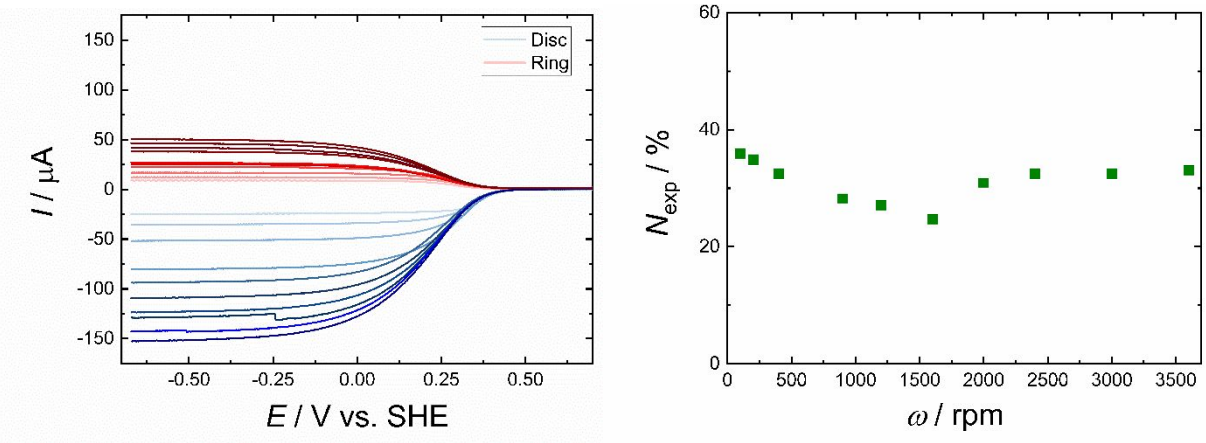

FigureS 15: a) LSV of 1 mM $K_3[Fe(CN)_6]$ at various rotation speeds ω between 100 and 3600 rpm b) Calculated experimental collection efficiencies N_{exp} thereof.

The plot of the calculated faradaic efficiencies for H_2O_2 production in Figure 4b is based on the following LSV's recorded under oxygen saturated conditions in 0.1 M $NaHSO_4$, 0.1 M phosphate buffer and 0.1 M NaOH in FigureS 16:

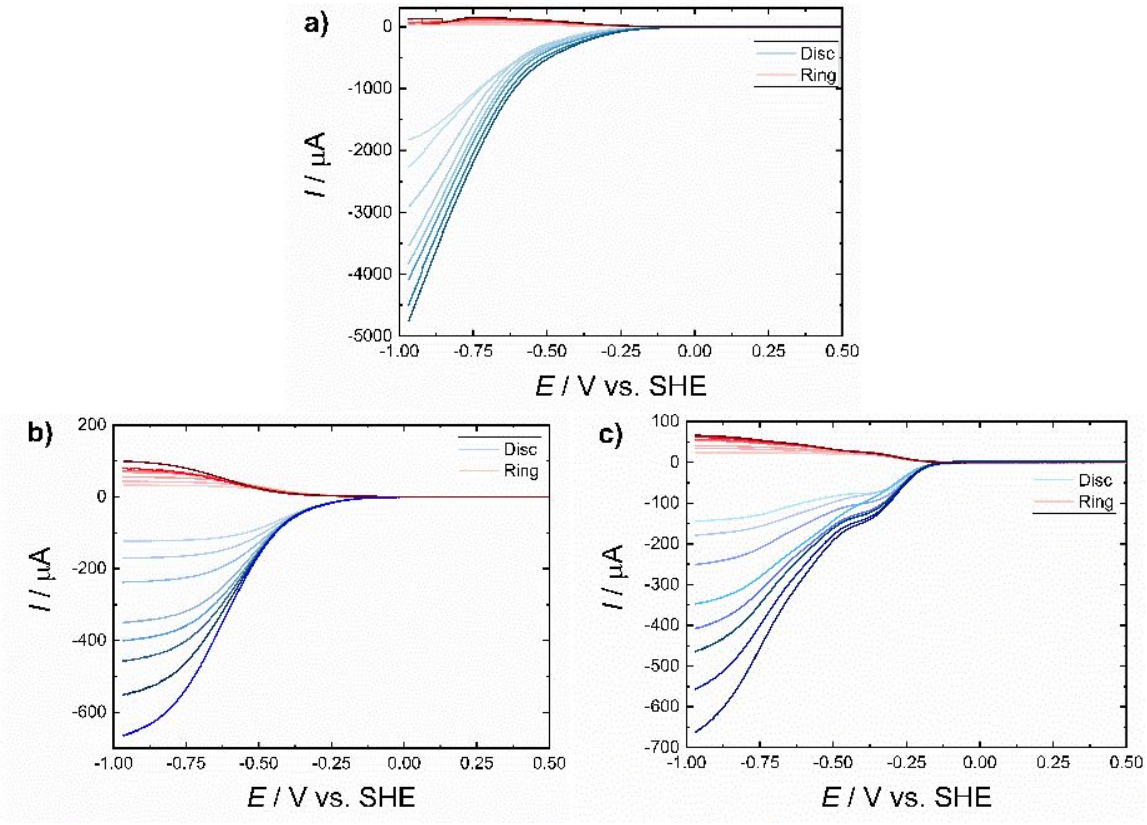

FigureS 16: LSV curves of GC/Pt RRDE recorded at a) pH 2, b) pH 7 and c) pH 13.

The LSV graphs of GC/PANI in 0.1 M $NaHSO_4$ (pH 2) under O_2 as well as with 5 mM H_2O_2 added are shown in the following FigureS 17:

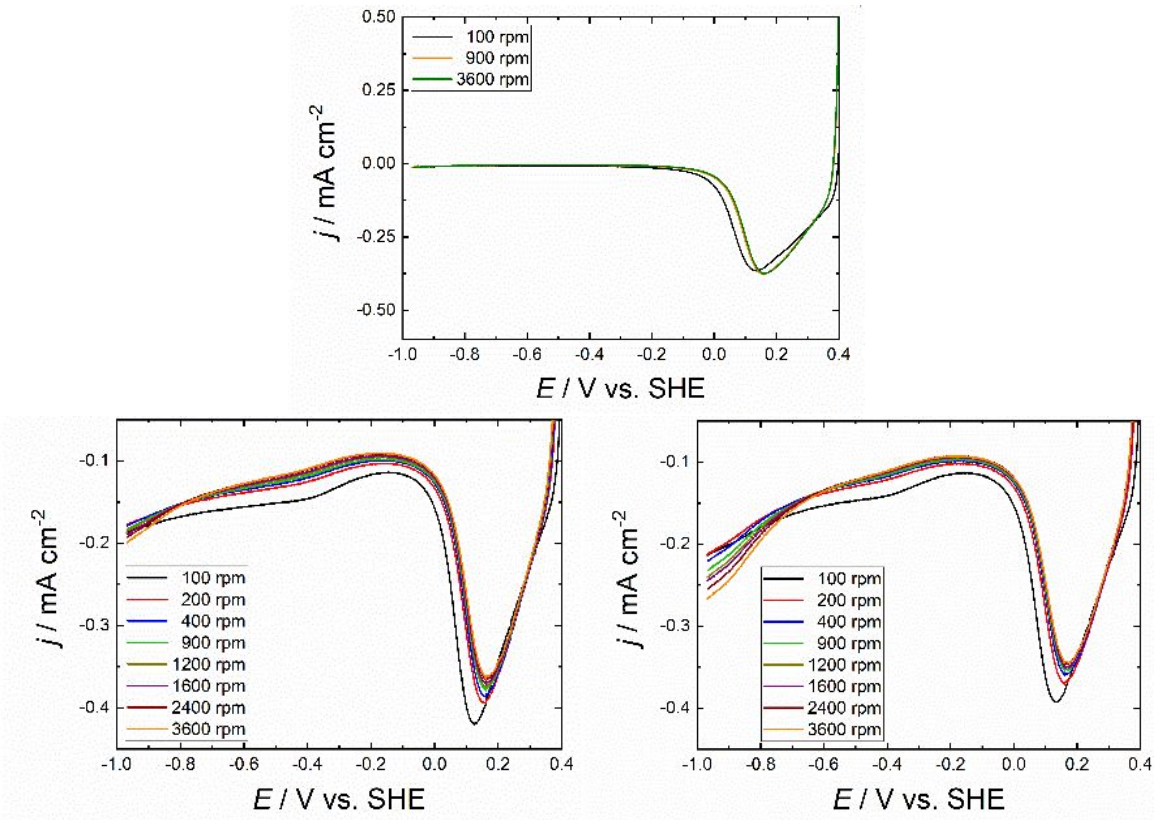

FigureS 17: LSV curves of a) GC/PANI at pH 2 under N_2, b) GC/PANI at pH 2 under O_2 and c)LSV curves of GC/PANI at pH 2 under O_2 with H_2O_2 added.

The LSV graphs of GC/PPy in 0.1 M $NaHSO_4$ (pH 2) as well as 0.1 M phosphate buffer (pH 7) under O_2 as well as with 5 mM H_2O_2 added are shown in the following FigureS 18:

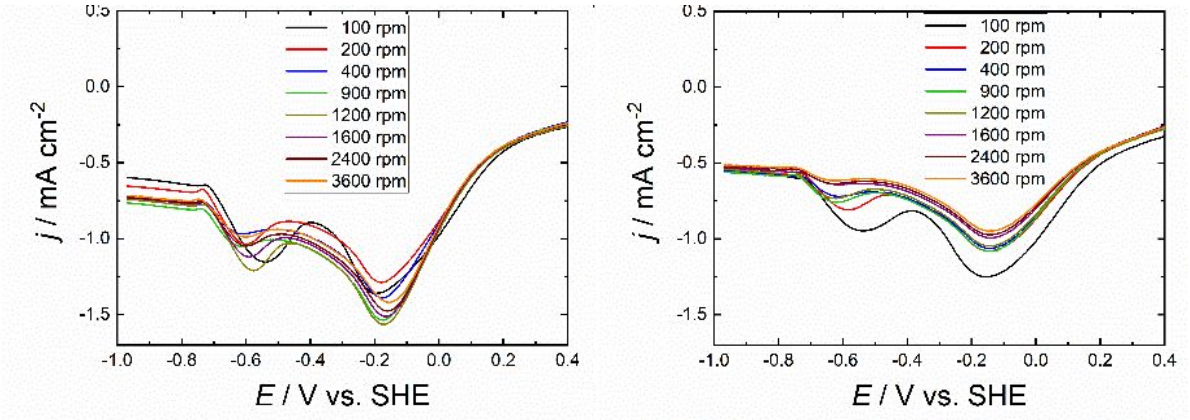

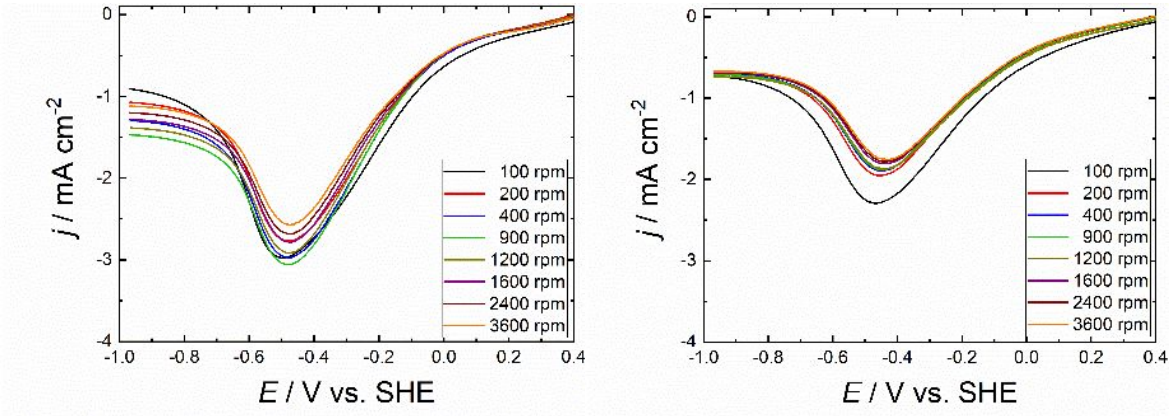

FigureS 18: LSV curves of a) GC/PPy at pH 2 under O_2, b) of GC/PPy at pH 2 under O_2 with H_2O_2 added, c) GC/PPy at pH 7 under O_2 and d) of GC/PPy at pH 7 under O_2 with H_2O_2 added.

References:

(1) Letheby, H. On the Production of a Blue Substance by the Electrolysis of Sulphate of Aniline. *J. Chem. Soc.* **1862**, *15*, 161–163. https://doi.org/10.1039/js8621500161.

(2) Nunziante, P.; Pistoia, G. Factors Affecting the Growth of Thick Polyaniline Films by the Cyclic Voltammetry Technique. *Electrochim. Acta* **1989**, *34* (2), 223–228. https://doi.org/10.1016/0013-4686(89)87089-6.

(3) Su, G.; Wei, Y.; Guo, M. Direct Colorimetric Detection of Hydrogen Peroxide Using 4-Nitrophenyl Boronic Acid or Its Pinacol Ester. *Am. J. Anal. Chem.* **2011**, *2*, 879–884. https://doi.org/10.4236/ajac.2011.28101.

(4) Apaydin, D. H.; Seelajaroen, H.; Pengsakul, O.; Thamyongkit, P.; Sariciftci, N. S.; Kunze-Liebhäuser, J.; Portenkirchner, E. Photoelectrocatalytic Synthesis of Hydrogen Peroxide by Molecular Copper-Porphyrin Supported on Titanium Dioxide Nanotubes. *ChemCatChem* **2018**, *10* (8), 1793–1797. https://doi.org/10.1002/cctc.201702055.

(5) Werner, D.; Griesser, C.; Stock, D.; Griesser, U. J.; Kunze-Liebhäuser, J.; Portenkirchner, E. Substantially Improved Na-Ion Storage Capability by Nanostructured Organic − Inorganic Polyaniline-TiO2 Composite Electrodes. *ACS Appl. Energy Mater.* **2020**, *3*, 3477–3487. https://doi.org/10.1021/acsaem.9b02541.

(6) Blinova, N. V.; Stejskal, J.; Trchová, M.; Prokeš, J.; Omastová, M. Polyaniline and Polypyrrole: A Comparative Study of the Preparation. *Eur. Polym. J.* **2007**, *43*, 2331–2341. https://doi.org/10.1016/j.eurpolymj.2007.03.045.

(7) Bard, A. J.; Faulkner, L. R. *Electrochemical Methods*, 2nd Ed.; John Wiley & Sons, Inc.: New York, 2001.

(8) Sun, Y.; Sinev, I.; Ju, W.; Bergmann, A.; Dresp, S.; Kühl, S.; Spöri, C.; Schmies, H.; Wang, H.; Bernsmeier, D.; Paul, B.; Schmack, R.; Kraehnert, R.; Cuenya, B. R.; Strasser, P.; Efficient Electrochemical Hydrogen Peroxide Production from Molecular Oxygen on Nitrogen-Doped Mesoporous Carbon Catalysts. *ACS Catal.* **2018**, *8*, 2844–2856. https://doi.org/10.1021/acscatal.7b03464.

(9) Sehrish, A.; Manzoor, R.; Dong, K.; Jiang, Y.; Lu, Y. Recent Progress on Electrochemical Production of Hydrogen Peroxide. *Chem. Reports* **2019**, *1* (2), 81–101. https://doi.org/10.25082/CR.2019.02.005.